Photoproduction at HERA with a Leading Proton

Hanna Mahlke-Krüger

H1 Collaboration, DESY

Abstract. The total cross-section for the semi-inclusive photoproduction process with a leading proton in the final state has been measured at centre-of-mass energies W between 91 and 231 GeV. The measured cross-sections refer to the kinematic range with transverse momenta of the scattered proton restricted to $p_T \leq 0.2\,\mathrm{GeV}$ and $0.66 \leq z \leq 0.90$, where $z = E'_p/E_p$ is the scattered proton energy normalized to the beam energy. The cross-section $\mathrm{d}\sigma_{\gamma p \to p' X}(W)/\mathrm{d}z$ is observed to be independent of the photon-proton centre-of-mass energy and the scattered proton momentum within the measurement errors and amounts to $8.00 \pm 0.42(stat) \pm 1.07(syst)\,\mu\mathrm{b}$ on average. The measured cross-sections are compared with semi-inclusive deep inelastic scattering data with a leading proton in the final state subjected to the same kinematic selection criteria. The semi-inclusive photoproduction cross section is suppressed more strongly than the semi-inclusive DIS cross section with respect to the inclusive data.

I INTRODUCTION

The HERA electron proton collider has allowed semi-inclusive cross sections of the form $\gamma^{(*)}p \to Xp'$ to be studied in detail for both real and virtual photons. In this paper, a measurement of the semi-inclusive cross-section of the photoproduction process is presented, which is combined with the corresponding data from deep inelastic scattering (DIS) processes [1]. The process under study is sketched in Figure 1.

The transition in reactions $\gamma^{(*)}p \to X$ from finite Q^2 to $Q^2 = 0$ is conveniently described by introducing a total virtual photon proton cross-section

$$\sigma^{tot}_{\gamma^{(*)}p}(W, Q^2) \approx \frac{4\pi^2\alpha}{Q^2} F_2(x, Q^2) \tag{1}$$

where $x = Q^2/(2p_p \cdot q)$ is the Bjorken scaling variable and p_p and q are the four-momenta of the incident proton and photon, respectively. α is the fine-structure constant and F_2 the proton structure function. W denotes the total $\gamma^* p$ centre-of-mass energy, which for the present application of small values of the scaling variable x can be approximated by $W^2 \approx Q^2/x$. The inelasticity of the process, y,

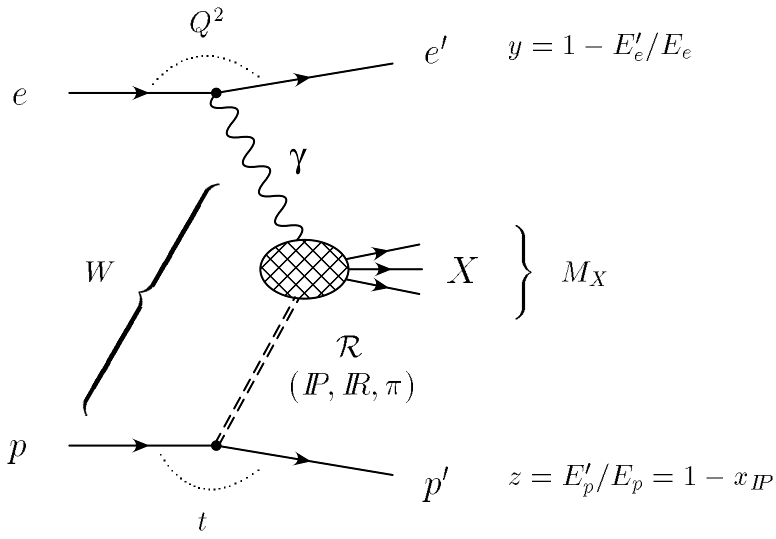

FIGURE 1. *The process $ep \to e'p'X$. At the proton vertex, $z = E'_p/E_p$ is the fractional momentum kept by the proton.*

is defined as $y = (p_p \cdot (p'_e - p_e))/(p_p \cdot p_e)$ with p_e and p'_e the four-momenta of the incoming and outgoing electron. In photoproduction, y can be measured using the relation $y = 1 - E'_e/E_e$, where E_e and E'_e indicate the energies of the incoming and outgoing electron, respectively. Here, for $\gamma^{(*)}p \to p'X$, the situation is viewed as follows: The photon dissociates to a system of mass M_X. The proton remains intact leaving the interaction with a fractional energy $z = E'_p/E_p$, where E'_p and E_p are the energies of the incident and scattered proton, respectively[1]. In the publication [1] DIS data in the kinematic range $0.71 \leq z \leq 0.90$ were shown to be well described by a Regge model in which the virtual photon interacts with colourless constituents of the proton. In Regge terminology, this corresponds to a hadronic exchange $\mathcal{R}$ colliding with the photon at fixed energy $(1-z)E_p$. In the kinematic range of this study, the pomeron contribution to $\mathcal{R}$ is suppressed relative to the exchange of pion or the degenerate trajectories of the ρ, ω, f, and a_2 exchange in this paper denoted by $I\!R$. The variables describing this process are $\beta = x/(1-z)$ instead of x and the invariant mass of the $\gamma\mathcal{R}$ system $M_X = W\sqrt{1-z}$. Note that for each value of z, the choice of W fixes M_X.

A comparison of semi-inclusive data with a leading proton in the final state at fixed z and finite values of Q^2 with data at $Q^2 = 0$ can be viewed as investigating the limit $Q^2 \to 0$ for $\gamma I\!R$ or $\gamma\pi$ reactions at fixed $\gamma\mathcal{R}$ CM energies. Assuming the proton and photon vertices can be factorised, the flux factors describing the probability of exchanging $\mathcal{R}$ at fixed z can be considered as a common normalisation parameter for photoproduction and DIS.

---

1) In some publications, $x_{I\!P} = 1 - z$ is used instead.

II APPARATUS AND DATA SELECTION

The H1 detector is described in detail elsewhere [2]. The direction of the incoming proton beam is labelled the forward direction and taken to be the $+z$ axis, the x axis points towards the centre of the storage rings, and the y axis points upwards relative to the plane of the HERA electron ring. The selection on the final state is performed by identifying the scattered proton, the scattered electron, and a charged track in the central region of the H1 detector. The analysis is based on a data set from the 1996 running period, where HERA collided 820 GeV protons with 27.5 GeV positrons, the integrated luminosity amounts to $3.3\,\mathrm{pb}^{-1}$.

The Forward Proton Spectrometer[2] (FPS) [3] is used to measure the energy and scattering angle at the interaction point of the outgoing proton. The error on the energy measurement is less than 8 GeV. The detector size, the distance of the detector stations from the interaction point, and the proton beam size restrict the acceptance in the proton's transverse momentum to $p_T \leq 0.2$ GeV. For the present analysis the energy range was restricted to $0.66 \leq z = E'_p/E_p \leq 0.90$, divided into five intervals. The measurement integrates over the accessible p_T range.

An electron was required to be found in one of the electron calorimeters, belonging to the luminosity system, which is used also for determination of the luminosity and background rejection due to Bethe-Heitler events. The acceptance is experimentally restricted to values of $Q^2 < 0.01\,\mathrm{GeV}^2$. The data sample was binned according to the value of the inelasticity $y = 1 - E'_e/E_e$, where E'_e is equal to the energy measured in the tagger calorimeters. The values for the mean γp centre-of-mass energy W, calculated as $W = \sqrt{ys}$, for the three bins are: $W_1 = 91$ GeV, $W_2 = 187$ GeV, $W_3 = 231$ GeV.

Furthermore, at least one reconstructed track inside the main H1 detector with $p_T^{\mathrm{trk}} > 500$ MeV, $20° < \theta < 160°$ was required. The effect of this acceptance cut was corrected using the PHOJET Monte Carlo program [4].

Further background rejection cuts were imposed.

III CROSS SECTION MEASUREMENT

The differential cross section $\mathrm{d}\sigma_{\gamma p \to Xp'}(W^2, E'_p)/\mathrm{d}z$ can be determined using the relation

$$\frac{\mathrm{d}^3\sigma_{ep\to eXp'}(W^2,Q^2,z)}{\mathrm{d}y\mathrm{d}Q^2\mathrm{d}z} = \mathcal{F}_{\gamma/e}(y,Q^2)\frac{\mathrm{d}\sigma_{\gamma p\to Xp'}(W^2,z)}{\mathrm{d}z}, \qquad (2)$$

where $\mathcal{F}_{\gamma/e}(y,Q^2)$ is the photon flux in the Equivalent Photon Approximation [5]. The data are corrected for acceptances and efficiencies. Further details can be found in [6].

---

2) The Forward Proton Spectrometer was supported by the INTAS93-43 project and the NATO contract PST.CLG.975100.

A Background

The following sources of background were studied:

- The contribution arising from events in which the proton signal in the final state is faked in the FPS is estimated to be on the percent level and neglected.
- Tracks in the central H1 detector produced by beam gas interactions: This background fraction has been determined to vary between 2.2 and 3.4%, depending on the y bin, and was subtracted.
- Bethe Heitler events $ep \to ep\gamma$: By experimental means it is verified that these events contribute only at the level of 0.25%. The background has been subtracted.

B Systematic errors

Three types of systematic errors are distinguished. These are errors common to events in the same y interval, errors related to the proton energy (or z) interval and global errors.

The following sources contribute to errors common to all events in the same y bin: background from proton beam gas interactions in the central region of the H1 detector, errors on the acceptance of the electron taggers, errors on the selection efficiency for tracks in the H1 tracking chambers, and migration correction between adjacent y bins. These errors vary between 6.5% and 8.5%.

Depending on the z bin, uncertainties between 2.6% and 14.1% are obtained, related to correction factors for migration and acceptance correction. The factors were determined using the PHOJET [4] and POMPYT [7] Monte Carlo generators.

Further contributions to the systematic error given by the uncertainty on the luminosity measurement, a value for FPS systematic errors such as alignment errors, uncertainty on the hodoscope efficiencies, and other effects not covered by the simulation, and additionally systematic errors on the vertex cut efficiency and positron beam related background give rise to 5.3% of systematic error to all bins.

C Results

The cross section $\mathrm{d}\sigma_{\gamma p \to p' X}(W)/\mathrm{d}z$ for $W = 91$, 187, and 231 GeV and five values of z for $0.66 \leq z \leq 0.90$ is shown in Figure 2. The errors shown are the square root of the quadratic sum of the systematic errors as described above and the statistical error. The total errors vary between 9.2% and 21.0%. No radiative corrections were applied to the data since they are expected to be negligibly small.

It is observed that in all z bins the measured cross-sections for different values of the γp centre-of-mass energy W agree with each other within the experimental errors. Furthermore the z dependence is only weak without a clear trend so that the present data may be represented by one average cross-section value of $\mathrm{d}\sigma(W,z)/\mathrm{d}z = 8.00 \pm 0.42(stat) \pm 1.07(syst)\,\mu$b (the measured values ranging between 7.2 and 9.4 μb) which corresponds to $\mathrm{d}\sigma(W,E_p')/\mathrm{d}E_p' \sim 9.76\,\mathrm{nb/\,GeV}$ for the kinematic range covered by this experiment. The restriction in the transverse momentum of the final state proton to $p_T \leq 0.2\,\mathrm{GeV}$ should be kept in mind, which is equivalent to the statement that the measured cross-section represents only about $(24 \pm 2)\%$ of the total semi-inclusive photoproduction cross-section if a slope of $b = (6.8 \pm 0.8)\,\mathrm{GeV}^{-2}$ in $\mathrm{d}\sigma/\mathrm{d}p_T^2 \sim e^{-bp_T^2}$ is assumed as measured by the ZEUS collaboration [8] for the kinematic range under study. The semi-inclusive photoproduction process with a proton proton of $0.66 \leq z \leq 0.90$ and $p_T < 200\,\mathrm{MeV}$ contributes 1% to the total photoproduction cross-section.

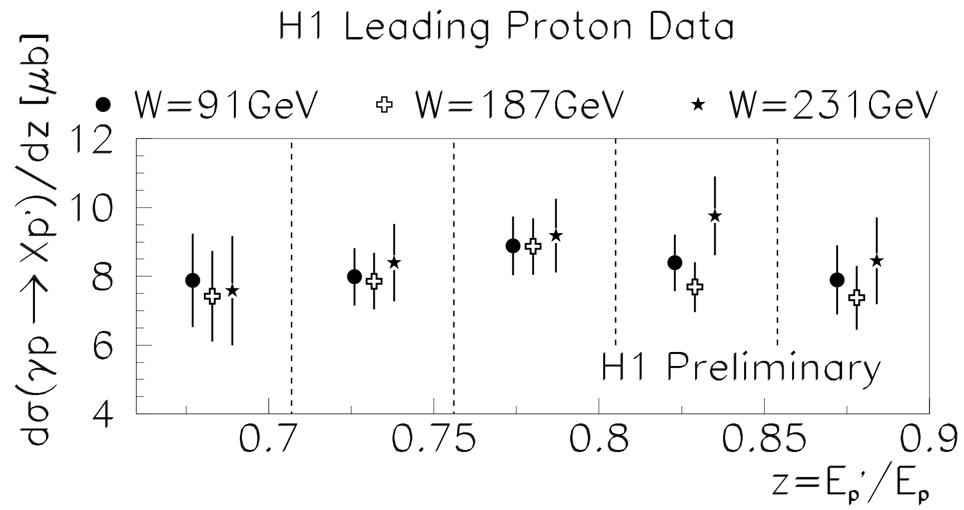

FIGURE 2. *The cross-section $d\sigma_{\gamma p \to p' X}/dz$ as a function of z for three values of W. The inner error bar is the statistical and the outer the total error (statistical and systematical error added in quadrature). The dashed lines show the limits of the z intervals over which the differential cross-sections are averaged.*

IV LEADING PROTON PRODUCTION IN DIS AND PHOTOPRODUCTION

Applying Equation (1), inclusive deep inelastic scattering and inclusive photoproduction data from the reaction $\gamma^{(*)}p \to X$ have been combined in order to study the transition between the two kinematic regimes in [9]. In the present paper, the same investigation is performed for the process $\gamma^{(*)}p \to p'X$.

For the semi-inclusive case, the deep inelastic structure function $F_2^{LP(3)}$ [1] is related to the leading proton photoproduction data as indicated below. The data points are displayed in Figure 3:

$$\frac{\mathrm{d}\sigma_{\gamma^{(*)}p\rightarrow p'X}(W^2,Q^2,z)}{\mathrm{d}z} = \frac{4\pi^2\alpha}{Q^2} F_2^{LP(3)}(W^2,Q^2,z). \tag{3}$$

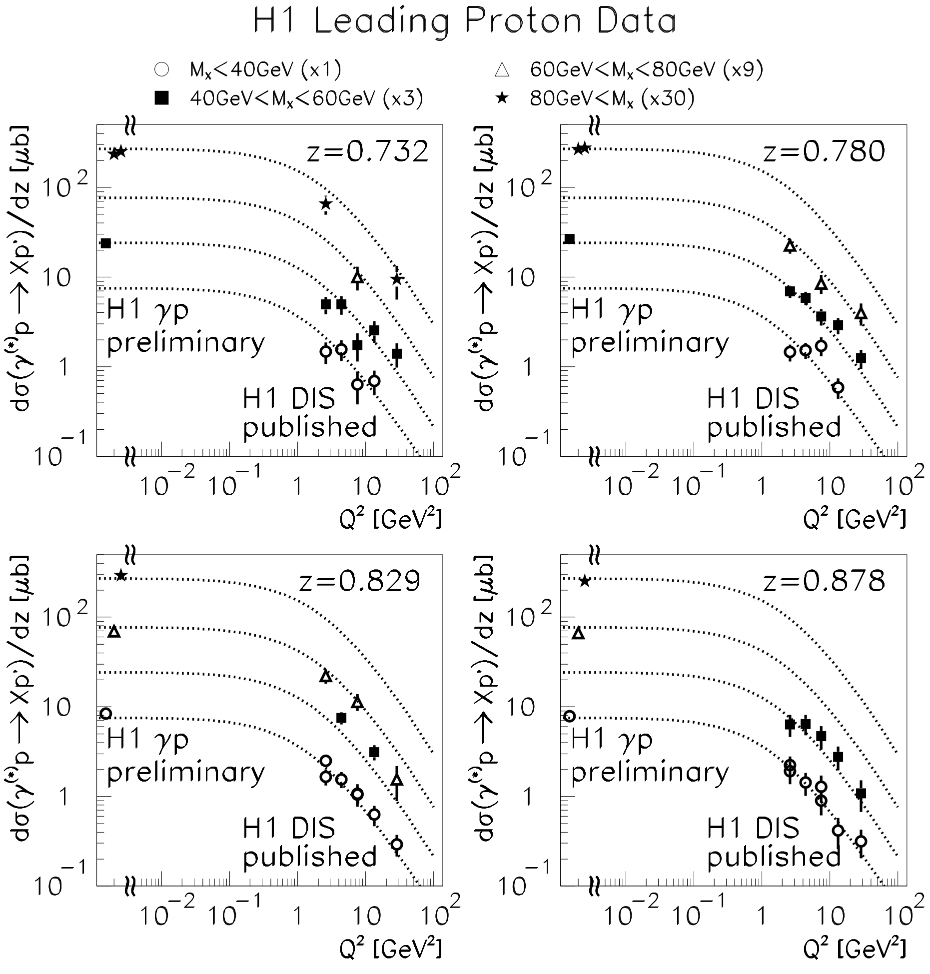

FIGURE 3. *The cross-section $d\sigma_{\gamma^{(*)}p\rightarrow p'X}/dz$ for four bins of z and four bins of M_X as a function of Q^2. The curves are the result of the fit described in the text.*

In [9] the inclusive data have been parametrized by a function inspired by the model described in [10], where the proton structure is assumed to consist of two components: F_2^{VDM} dominant at low values of the photon virtuality describing the contribution of vector mesons coupling to the virtual photon [11], and a partonic structure function F_2^{part}, governing the region $Q^2 > 1\,\mathrm{GeV}^2$ [10], which can be taken from a structure function measurement.

The model of [10] has not been developed to cover reactions with a leading proton, which according to the diagram of Figure 1 corresponds to a situation where the real or virtual photon interacts with a colourless constituent of the proton and not with the proton. However, an argument can be made that the exchanged object itself has a partonic structure, such that the VDM part describes a vector meson on reggeon or pion scattering process. A similar ansatz is used here. Therefore, making use of the observation that the deep inelastic semi-inclusive cross-section is also nearly independent of W and z, two additional parameters are introduced. A common scale factor F absorbs the flux factor for the probability to find $\mathcal{R}$ in the proton. This factor is assumed to be independent of Q^2 at fixed z and is a compensation for the reduction in phase space due to the limited transverse momentum of the scattered protons. A further normalization factor C_{VM}^{LP} for the vector meson contribution is assumed. The variable replacing x of the inclusive case is $\beta = x/(1-z)$. The parameters introduced in [9] were used with the values determined in that paper.

For the structure function of $\mathcal{R}$, we use the VDM and QCD parameterisation for the proton, implicitly assuming that hadronic structure functions have the same behaviour at low x, up to a normalisation. This normalisation is absorbed into the common scale factor, for which a value $F = 0.124 \pm 0.011(stat) \pm 0.010(syst)$ is obtained. The result for the relative normalization factor is $C_{VM}^{LP} = 0.16 \pm 0.08$.

It is thus observed that the VDM term is suppressed by a factor of 0.16 with respect to the inclusive case. This is significantly smaller than the factor of 2/3 between the total cross-sections for pion proton and proton proton scattering, which one would expect to be applicable if cross-sections were related to the number of valence quarks involved in a particular reaction.

The fits are displayed in Figure 3 together with the DIS and photoproduction data points. As in the case of inclusive reactions, the fits suggest a transition near $Q^2 \approx 1\,\mathrm{GeV}^2$, where the DIS cross-section turns over into a non-scaling regime and approaches the photoproduction value.

V SUMMARY

Photoproduction reactions with a final state proton of $p_T \leq 0.2\,\mathrm{GeV}$ observed in the H1 Forward Proton Spectrometer have been analysed in the kinematic range $0.66 \leq z \leq 0.90$ at γp centre-of-mass energies $W = 91$, 187 and 231 GeV. The cross-section $\mathrm{d}\sigma(W)/\mathrm{d}z$ was determined to be on average $8.00 \pm 0.42(stat) \pm 1.07(syst)\,\mu\mathrm{b}$, independent of z and W within the experimental errors.

The combination of data from photoproduction and deep inelastic scattering with a final state proton observed in the FPS, $\gamma^{(*)}p \rightarrow p'X$, in the kinematic range $0.71 \leq z \leq 0.90$ shows a qualitatively similar behaviour as observed when going from virtual to real photons in the inclusive reaction $\gamma^{(*)}p \rightarrow X$. A parametrization where the contributions to the cross-section are divided into a VDM and a partonic component shows a fair description of the data, provided the overall normalization and the relative normalization between the two components are adjusted. The fit indicates that the semi-inclusive cross-section for photoproduction is more strongly suppressed than the semi-inclusive DIS cross-section with respect to the inclusive data.

REFERENCES

1. H1 Collaboration, C. Adloff et al., *Eur. Phys. J.* **C 6** (1999) 587
2. H1 Collaboration, I. Abt et al., *Nucl. Instrum. Methods* **A 386** (1997) 310
3. P. Van Esch et al., *Nucl. Instrum. Methods* **A 446** (2000) 409
4. R. Engel, "PHOJET manual (Program version 1.05c, June 96)", University of Siegen preprint 95-05 (1995) (revised Feb. 96)
5. S. Frixione et al., *Phys. Lett.* **B 319** (1993) 330
6. H. Mahlke-Krüger, Dissertation Universität Hamburg, 1999
   H1 Collaboration, *paper in preparation*
7. P. Bruni, A. Edin, G. Ingelman, "POMPYT version 2.6 – A Monte Carlo Program to Simulate Diffractive Hard Scattering Processes", unpublished program manual (1996), see `http://www3.tsl.uu.se/thep/pompyt`
8. ZEUS Collaboration, in "Proceedings of ICHEP98 Conference, Vancouver", p. 924, World Scientific A. Astbury et al. ed., World Scientific (1998)
9. H1 Collaboration, C. Adloff et al., *Nucl. Phys.* **B 497** (1997) 3
10. B. Badełek, J. Kwieciński, *Phys. Lett.* **B 295** (1992) 263
11. J.J. Sakurai, D. Schildknecht, *Phys. Lett.* **B 40 No. 1** (1972) 121